

Chapter 28

MODIS-Derived Terrestrial Primary Production

Maosheng Zhao, Steven Running, Faith Ann Heinsch,
and Ramakrishna Nemani

Abbreviations

AmeriFlux	Eddy flux tower network of North America
Aqua	NASA's earth observing system satellite with afternoon equatorial crossing time
BIOME-BGC	A process-based biogeochemistry model developed by NTSG, University of Montana
BPLUT	Biome Properties Lookup Table
B_r	Base respiration value
C3	Collection or version 3 of MODIS data
C4	Collection or version 4 of MODIS data
C4.8	Collection or version 4.8 of MODIS GPP/NPP data
C5	Collection or version 5 of MODIS data
CDR	Climate data record
ENSO	El Niño-Southern Oscillation
ERA-40/ECMWF	A 40-year long-term meteorological reanalysis dataset generated by European Center for Medium range Weather Forecasting (ECMWF)
ESDR	Earth system data record
FAO	Food and Agriculture Organization of the United Nations
FLUXNET	Global eddy flux tower network
FPAR	Fraction of PAR
FTP	File transfer protocol
GEOS4	Name and version of assimilation system of GMAO
GMAO	Global modeling and assimilation office belonging to NASA
GPP	Gross primary production ($\text{g C/m}^2/\text{d}$)

M. Zhao (✉)

Numerical Terradynamic Simulation Group, University of Montana,
Missoula, MT 59812 USA
e-mail: zhao@ntsg.umt.edu

HDF-EOS	An extended Hierarchical Data Format for storing NASA's earth observing system data
ITCZ	Intertropical Convergence Zone
LAI	Leaf Area Index
LP-DAAC	Land Processes Distributed Active Archive Center
M_l	Living biomass for leaves and fine roots ($g C/m^2$), derived from LAI
MOD12Q1	MODIS land cover dataset
MOD15A2	8-day MODIS FPAR/LAI dataset
MOD17	MODIS GPP/NPP dataset
MOD17A2	8-day MODIS GPP/PsnNet dataset
MOD17A3	Annual MODIS GPP/NPP dataset
MODIS	Moderate Resolution Imaging Spectroradiometer, an instrument on board NASA's TERRA and Aqua satellite
NARR	North American Regional Reanalysis
NASA	The National Aeronautics and Space Administration
NCDC	National Climatic Data Center
NCEP/NCAR	National Centers for Environmental Prediction/National Center for Atmospheric Research
NDVI	Normalized Difference Vegetation Index
NH	North hemisphere
NPOESS	National Polar-orbiting Operational Environmental Satellite System
NPP	Annual net primary production ($g C/m^2/yr$)
NTSG	Numerical Terradynamic Simulation Group at University of Montana
NU_g	The number of days during the growing season with unreliable or missing MODIS LAI inputs
PAR	Photosynthetically active radiation
PsnNet	Net photosynthesis, an intermediate variable between GPP and NPP
Q_{10}	Respiration quotient, equal to 2.0
QC	Quality control data field for MODIS data
R_g	Annual growth respiration ($g C/m^2/yr$)
R_{m_lr}	Maintenance respiration from living leaves and fine roots ($g C/m^2/d$)
R_{m_w}	Annual maintenance respiration from living wood ($g C/m^2/yr$)
R_{plant}	Plant respiration, functionally, it is the summation of maintenance and growth respiration
$S\downarrow_s$	Downward surface solar shortwave radiation ($MJ/m^2/d$)
SLA	Specific leaf area
SOGS	Surface Observation gridding system
T_{avg}	Daily average air temperature ($^{\circ}C$)
Terra	NASA's earth observing system satellite with morning equatorial crossing time

T_f	Daily minimum temperature scalar
T_{\min}	Daily minimum temperature
TOTAL _g	Total number of days in the growing season
VIIRS	Visible/Infrared Imager/Radiometer Suite onboard NPOESS
VPD _f	Vapor pressure deficits (VPD) scalar
ϵ	Light use efficiency parameter (g C /MJ)
ϵ_{\max}	Maximum ϵ under optimal conditions (g C /MJ)

28.1 Introduction

Temporal and spatial changes in terrestrial biological productivity have a large impact on humankind because terrestrial ecosystems not only create environments suitable for human habitation, but also provide materials essential for survival, such as food, fiber and fuel. A recent study estimated that consumption of terrestrial net primary production (NPP; a list of all the acronyms is available in the appendix at the end of the chapter) by the human population accounts for about 14–26% of global NPP (Imhoff et al. 2004). Rapid global climate change is induced by increased atmospheric greenhouse gas concentration, especially CO₂, which results from human activities such as fossil fuel combustion and deforestation. This directly impacts terrestrial NPP, which continues to change in both space and time (Melillo et al. 1993; Prentice et al. 2001; Nemani et al. 2003), and ultimately impacts the well-being of human society (Milesi et al. 2005). Additionally, substantial evidence show that the oceans and the biosphere, especially terrestrial ecosystems, currently play a major role in reducing the rate of the atmospheric CO₂ increase (Prentice et al. 2001; Schimel et al. 2001). NPP is the first step needed to quantify the amount of atmospheric carbon fixed by plants and accumulated as biomass. Continuous and accurate measurements of terrestrial NPP at the global scale are possible using satellite data. Since early 2000, for the first time, the MODIS sensors onboard the Terra and Aqua satellites, have operationally provided scientists with near real-time global terrestrial gross primary production (GPP) and net photosynthesis (PsnNet) data. These data are provided at 1 km spatial resolution and an 8-day interval, and annual NPP covers 109,782,756 km² of vegetated land. These GPP, PsnNet and NPP products are collectively known as MOD17 and are part of a larger suite of MODIS land products (Justice et al. 2002), one of the core Earth System or Climate Data Records (ESDR or CDR).

These products have improved based on extensive validation and calibration activities by the MODIS science team. The Collection-5 (C5) MODIS data are being reprocessed by NASA in 2007 and will have higher quality than the previous collections. In this chapter, we provide a brief description of the global MODIS terrestrial primary production algorithm and data products, and summarize the achievements (i.e., validation, improvements, and applications) and results of a six-year (2000–2005) global MODIS GPP/NPP dataset.

28.2 Description of MODIS GPP/NPP

28.2.1 Theoretical Basis of the Algorithm

MODIS GPP/NPP is the first continuous satellite-derived dataset monitoring global vegetation productivity. The algorithm is based on Monteith's (1972, 1977) original logic, which suggests that NPP under non-stressed conditions is linearly related to the amount of absorbed Photosynthetically Active Radiation (PAR) during the growing season. In reality, vegetation growth is subject to a variety of stresses that tend to reduce the potential growth rate. Especially important are climatic stresses (temperature, radiation, and water) or the interaction of these primary abiotic controls, which impose complex and varying limitations on vegetation activity globally (Churkina and Running 1998; Nemani et al. 2003; Running et al. 2004). Figure 28.1 illustrates the range of three dominant climatic controls on global annual NPP, distributed from arctic tundra to tropical rainforests. Water limits vegetation most strongly on 40% of the land surface. Temperature is most limiting for 33% of the land surface, with annual temperature ranges from -20°C in arctic tundra to $+30^{\circ}\text{C}$ in deserts. Incident solar radiation is the primary limiting factor for 27% of global vegetated areas, mostly in wet tropical regions where temperatures and water availability are usually adequate (Nemani et al. 2003). While it is easy to imagine boreal areas being temperature-limited, and deserts being water-limited, partial constraints limit NPP of temperate regions in a complex fashion at different times of the growing season. A temperate mid-latitude forest is perhaps limited by radiation and temperature in winter, temperature-limited in the spring, and water-limited in mid-summer

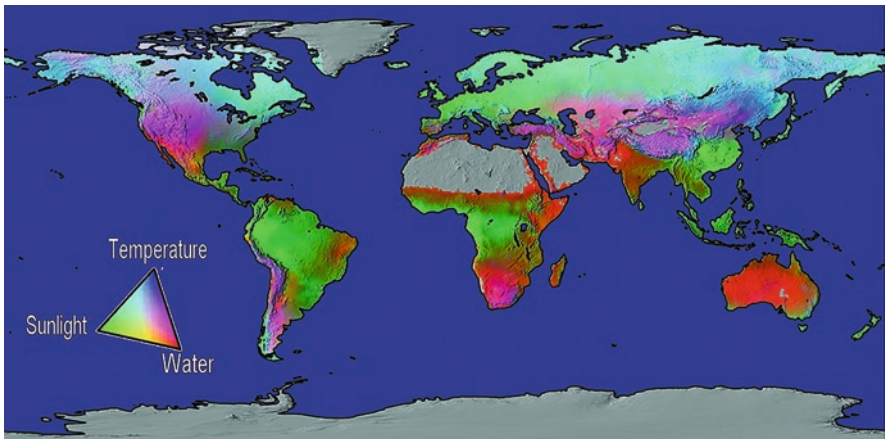


Fig. 28.1 Potential limits to vegetation net primary production based on fundamental physiological limits imposed by solar radiation, water balance, and temperature (from Churkina and Running 1998; Nemani et al. 2003; Running et al. 2004). Land regions with *gray color* are barren, sparsely vegetated and non-vegetated areas

(Jolly et al. 2005a). In addition to the abiotic constraints, another cost associated with the growth and maintenance of vegetation is called autotrophic respiration (Ryan 1991). Combining Monteith's logic, climate control, and some principles of modeling NPP learned from a general process-based ecosystem model, Biome-BGC (Running and Hunt 1993), the MODIS GPP/NPP algorithm was developed with satellite-derived data inputs. They include land cover, the fraction of photosynthetically active radiation absorbed by vegetation (FPAR), and leaf area index (LAI) as surface vegetation inputs (Running et al. 2000). Climate information is obtained from a NASA Goddard Global Modeling and Assimilation Office (GMAO)-developed global climatic data assimilation system.

28.2.2 The Algorithm

The daily GPP in the algorithm is calculated using the equation,

$$\text{GPP} = \text{PAR} \times \text{FPAR} \times \varepsilon \quad (28.1)$$

where ε is the light use efficiency, FPAR is the fraction of absorbed PAR, and PAR accounts for approximately 45% of incident shortwave solar radiation ($S \downarrow_s$), such that

$$\text{PAR} = S \downarrow_s \times 0.45 \quad (28.2)$$

The light use efficiency, ε , is derived by the reduction of the potential maximum, ε_{\max} , as a result of low temperatures (T_f) or limited water availability (VPD_f),

$$\varepsilon = \varepsilon_{\max} \times T_f \times \text{VPD}_f \quad (28.3)$$

The daily *PsnNet* is calculated as what remains once maintenance respiration from leaves and roots (R_{m_lr}) is subtracted from GPP,

$$\text{PsnNet} = \text{GPP} - R_{m_lr} \quad (28.4)$$

The original MODIS algorithm calculated growth respiration (R_g) as a function of annual maximum LAI, which may pose problems for many forests (see details in Sect. 28.5). As a result, for a given forest biome type R_g is invariable across both space and time, which is unreasonable according to plant physiological principles (Ryan 1991; Cannell and Thornley 2000). We have, therefore, modified it by assuming growth respiration is approximately 25% of NPP (Ryan 1991; Cannell and Thornley 2000) for C5 MOD17. Finally, annual NPP is computed as

$$\text{NPP} = 0.8 \times \sum_{i=1}^{365} (\text{PsnNet} - R_{m_w}) \quad (28.5)$$

where R_{m_w} is the maintenance respiration of live wood.

All maintenance respiration terms are calculated according to standard Q_{10} theory, which depends on the average ambient air temperature for leaves (Ryan 1991),

$$R_m = M_r \times B_r \times Q_{10}^{[(T_{avg} - 20)/10]} \quad (28.6)$$

where R_m refers to R_{m_lr} or R_{m_w} ; M_r is the living biomass in units of carbon for leaves, fine roots, or live wood, and B_r is the base respiration value, which is biome type-dependent. Leaf biomass is calculated using specific leaf area (SLA), while fine root biomass is calculated by multiplying the leaf biomass by the ratio of fine root to leaf biomass. This calculation is based on the assumption that the ratio between the fine root mass and leaf mass is constant. The live wood biomass is calculated using the annual maximum leaf biomass, and assumes that the ratio of live wood mass to leaf mass is constant for a given biome. Both these ratios are biome dependent. T_{avg} is daily average temperature. We assume Q_{10} has a constant value of 2.0 for both fine roots and live wood. For leaves, we have adopted a temperature-acclimated Q_{10} equation proposed by Tjoelker et al. (2001),

$$Q_{10} = 3.22 - 0.046 \times T_{avg} \quad (28.7)$$

The parameters for (28.3)–(28.6) are stored in a table called the Biome Properties Lookup Table (BPLUT). More details on the algorithm and data product format for both the 8-day and annual products are available in the MODIS GPP/NPP Users' Guide (Heinsch et al. 2003).

28.2.3 Data Flow and Products

Figure 28.2 provides a flowchart of the logic of the MODIS GPP and NPP algorithm, demonstrating how daily GPP and annual NPP are calculated with MODIS land cover, FPAR, and LAI, as well as the GMAO daily meteorological dataset. The 8-day MODIS GPP and PsnNet values for each pixel are actually the sum of the variables for the 8-day period, which are stored in the 8-day MOD17A2 product. Correspondingly, there is a quality control (QC) variable, which denotes whether the input 8-day FPAR/LAI is contaminated (e.g., by clouds) or reliable. The annual product (MOD17A3) includes annual total (i.e., summation of) GPP and NPP and the accompanying QC (for the definition of the annual QC, please see Sect. 28.5). Both MOD17A2 and MOD17A3 are stored in HDF-EOS format, which is a self-describing data format with ancillary metadata information, such as variable names, units, offset and gain, and other relevant data.

One of the unique features of MODIS GPP and NPP is that they represent the summation of carbon absorbed by vegetation, which differs from other MODIS

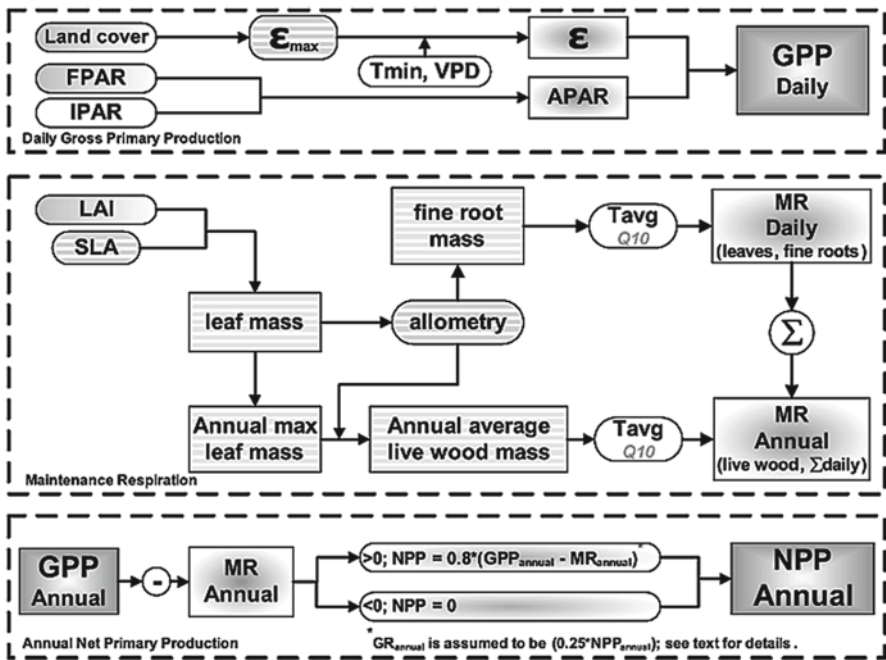


Fig. 28.2 Flowchart showing the logic behind the MOD17 Algorithm used to calculate both 8-day average GPP and annual NPP

vegetation products, such as the vegetation indices, FPAR, and LAI. Vegetation indices and FPAR/LAI are 8-day or 16-day maximum value composited data; there are no associated annual products. If there are missing data or data of poor quality resulting from contamination by cloud cover or severe atmospheric aerosol, users must fill the gaps with a method appropriate to their needs. However, for both 8-day and annual MOD17, if users want to fill the contaminated or missing gaps they must, theoretically, first gap-fill the FPAR and LAI, and then compute the MOD17 products using the MOD17 algorithm and corresponding daily meteorological data. This poses a potentially prohibitive obstacle to users. To solve this problem, we generate an improved MOD17 at the University of Montana and provide the data on our FTP site for users to freely download. The data format is similar to that of the official products to eliminate confusion. As a result, there are several options for users to obtain MOD17, depending on their needs. Users can get the near real-time 8-day MOD17A2, with gaps, through the Land Processes Distributed Active Archive Center (LP-DAAC), or they can get our reprocessed, quality-control filtered, and gap-filled 8-day and annual MOD17 through our FTP site at the end of the processing year. Section 28.5 details the method used to fill gaps in the MODIS FPAR/LAI inputs to reprocess the improved MOD17.

28.3 Input Uncertainties and the Algorithm

Three sources of MOD17 inputs exist (Fig. 28.2). For each pixel, biome type information is derived from MODIS land cover products (MOD12Q1); daily meteorological data are derived from the GMAO dataset; and 8-day FPAR and LAI are obtained from MOD15A2. The uncertainties in GMAO, MOD12Q1, MOD15A2, and the algorithm itself all influence MOD17 results.

The GMAO is an assimilated meteorological dataset, not observed data. As a result, it may contain systematic errors in some regions. At the global scale, we have found that the largest uncertainty for MOD17 derives from the global meteorological re-analysis data. We evaluate uncertainties in the three well-documented global re-analyses, including GMAO/NASA, ERA-40/ECMWF, and NCEP/NCAR, and how these uncertainties propagate to MOD17. To do so, we comprehensively compare the four main surface meteorological variables, surface downward solar radiation ($S\downarrow_s$), air temperature (T_{avg}), air vapor pressure (e_a), and vapor pressure deficit (VPD) from the three re-analyses datasets with surface weather station observations. We evaluated how the uncertainties in these re-analyses affect the MOD17 algorithm-derived NPP estimates (Zhao et al. 2006).

Our study showed that NCEP tends to overestimate $S\downarrow_s$, and underestimate both T_{avg} and VPD . ECMWF has the highest accuracy but its radiation is lower in tropical regions than NCEP, and GMAO's accuracy lies between NCEP and ECMWF. Temperature biases are mainly responsible for the large biases in VPD in the re-analyses data, because of VPD 's dependence on temperature. Figure 28.3 shows the patterns of zonal means and totals of MODIS GPP and NPP estimated by different re-analyses. MODIS NPP contains more uncertainties than GPP. Global total MODIS GPP and NPP driven by GMAO, ECMWF and NCEP show notable differences (>20 Pg C/yr) with the highest estimates from NCEP and the lowest from ECMWF. Again, the GMAO results lie somewhere between the NCEP and ECMWF estimates. Spatially, the larger discrepancies among the re-analyses and their derived MODIS GPP and NPP occur in the tropics. These results reveal that the biases in meteorological re-analyses datasets can introduce substantial error into GPP/NPP estimates, and emphasize the need to minimize these biases to improve the quality of MODIS GPP/NPP products (Zhao et al. 2006).

Land cover (MOD12Q1) accuracies fall in the range of 70–80%, and most “mistakes” are between similar classes (Strahler et al. 2002). A misclassified land cover pixel will likely lead to a misuse of MOD17 BPLUT parameters, which leads to less reliable MOD17 results. In addition, the current 1-km MODIS global land cover classification unit is probably too general for local application. Croplands, for example, are very diverse, yet the same set of parameters is applied indiscriminately to croplands everywhere, introducing large uncertainties for some crops in some regions.

A pixel-by-pixel comparison of MOD15A2 with ground measurements has a poor correlation, and retrieved LAI values have a propensity for overestimation under most conditions (Wang et al. 2004; Abuelgasim et al. 2006; Heinsch et al.

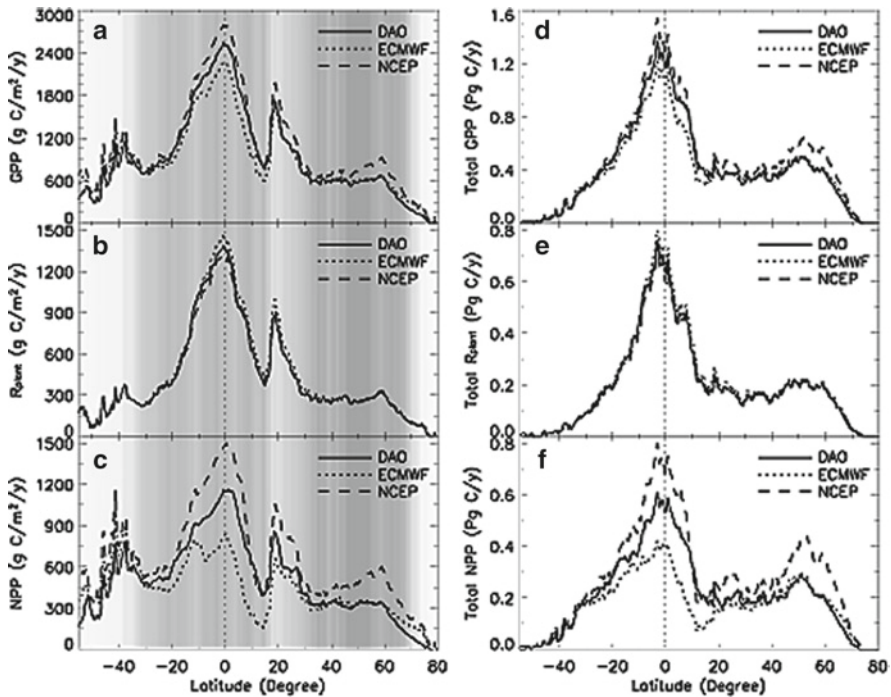


Fig. 28.3 Comparison of the zonal mean of annual GPP, R_{plant} , and NPP (a–c), and corresponding zonal totals (d–f) driven by the three re-analyses for 2000 and 2001 after aggregation into 0.5° intervals. The vegetated land area is shown as a gray scale, where darker shades represent more vegetation (Zhao et al. 2006)

2006; Pandya et al. 2006). Comparison at the patch level can significantly improve the results, but retrieved LAI are still inclined to produce higher values (Wang et al. 2004). In the MOD17 algorithm, FPAR is directly related to photosynthetic assimilation, and LAI is only related to autotrophic respiration. Therefore, an overestimated LAI from MOD15A2 may result in an underestimated NPP even if FPAR is relatively accurate. Although the temporal filling of unreliable FPAR/LAI greatly improves the accuracy of inputs, as discussed in Sect. 28.5, the filled values are artificial and contain uncertainties, and their quality is determined by the accuracy of FPAR/LAI without contamination in the temporal profile.

Finally, weaknesses in the MOD17 algorithm may lead to uncertainties in GPP/NPP. For example, the potential maximum value and realistic value under environmental controls for light use efficiency (ϵ), a key physiological variable, is still difficult to determine globally. GPP estimated from eddy flux towers can provide valuable information on ϵ (Turner et al. 2003a) and is useful to calibrate ϵ in the algorithm (Reichstein et al. 2004; Turner et al. 2005; Zhao et al. 2005). However, current studies are limited to a few sites, and more extensive studies are needed

to conduct the analysis across the global flux network. In addition, we still have little information regarding the actual values of other parameters in the BPLUT, such as fine root maintenance respiration base, and the biomass ratio of fine roots to leaves. Currently, for a given biome type, the same suite of parameters is being used without spatial variation, which may create uncertainties for some regions or specific plant species. Plant respiration algorithms also contain large uncertainties besides those in the input data since we do not yet fully understand plant respiration (Amthor 2000).

28.4 Validation

Validation to identify problems is our first priority because algorithm refinement and BPLUT calibration cannot take place. The BigFoot Project (<http://www.fsl.orst.edu/larse/bigfoot/index.html>) was organized specifically to address MODIS product validation needs for both the MOD15 LAI and the MOD17 GPP/NPP products, and our participation in the Bigfoot project has provided valuable assessment of the MODIS LAI, FPAR, GPP and NPP products. Figure 28.4 shows the logic used for MOD17 validation with AmeriFlux towers, including nine sites in agriculture, temperate mixed forest, semi-arid coniferous forest, boreal needle-leaf forest, Arctic tundra, desert grassland, prairie grassland, southern boreal mixed forest, and moist tropical broadleaf forest (Turner et al. 2006b). Measurements at these sites include field LAI, above-ground NPP, and net ecosystem CO₂ exchange (to estimate GPP) under a carefully-designed sampling scheme for a 7 × 7-km area specifically chosen to allow scaling with geostatistical theory to the MODIS datasets (Cohen et al. 2003). Maximum values, seasonality, and annual total values were estimated for comparison with MODIS data, and a number of papers were published in support of this activity, most recently those by Cohen et al. (2006) and Turner et al. (2005, 2006a, b).

Validation of weekly GPP is important to determine the accuracy of the MOD17 algorithm. As a result, we are developing relationships with researchers who participate in the FLUXNET network of eddy covariance flux towers, which AmeriFlux is a member of for the purpose of comparing MODIS GPP estimates with flux tower estimates (Running et al. 1999; Baldocchi et al. 2001; Falge et al. 2002; Heinsch et al. 2006). Fifteen sites participated fully in the validation effort, and results indicate that MODIS does a reasonable job of predicting GPP over various biomes throughout North America at 1-km resolution ($r = 0.86 \pm 0.17$ [95% confidence limit], Fig. 28.5a), although its accuracy varies by biome type (Heinsch et al. 2006). Much of the variation between tower and MODIS GPP arises from the use of coarse resolution GMAO input data ($28 \pm 45\%$), with much of that error derived from estimates of VPD and incoming shortwave solar radiation. Although the MOD17 GPP algorithm was parameterized specifically for use with

FLUX TOWER-BASED VALIDATION FOR MODIS GPP/NPP

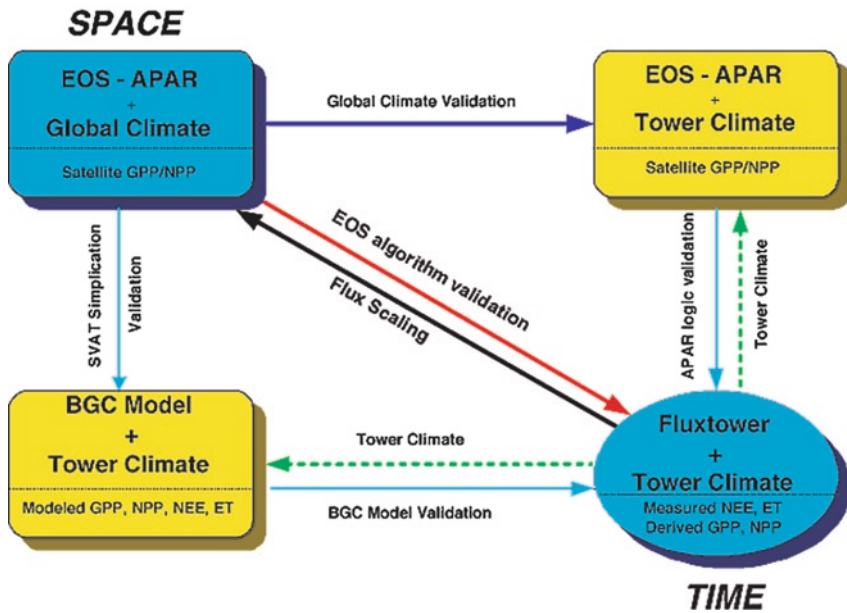


Fig. 28.4 The organizing logic we follow to validate MOD17 GPP with flux tower data, where tower meteorology, ground-measured FPAR, and more rigorous ecosystem models are sequentially substituted to evaluate sources of error and variability in MOD17 (based on Running et al. (1999))

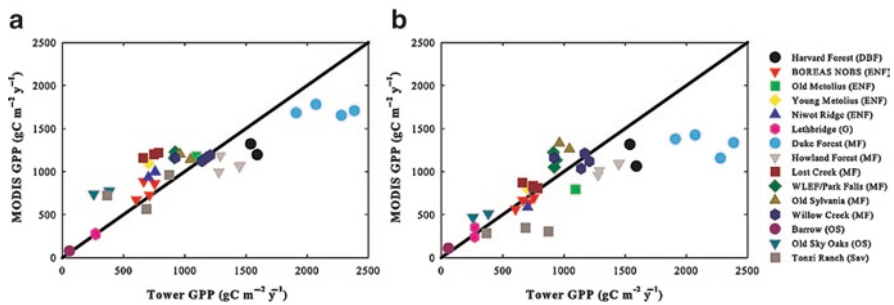


Fig. 28.5 Comparison of the annual MODIS GPP with flux tower-measured GPP for 15 AmeriFlux sites for 2001. These data were created using (a) the global GMAO meteorological data as driver and (b) tower-specific meteorology (Heinsch et al. 2006)

coarse resolution meteorology, using tower meteorology with the MOD17 algorithm suggests the main GPP algorithm is fairly accurate as well ($r = 0.79 \pm 0.21$ [95% confidence limit], Fig. 28.5b).

28.5 Processing Improvements and the Algorithm

Four major issues in the collection-4 (C4) MOD17 reprocessing exist:

1. The C4 MOD17 operational process fails to account for the mismatched spatial resolution between a 1-km MODIS pixel and the corresponding $1.00^\circ \times 1.25^\circ$ GMAO meteorological data.
2. The C4 MOD17 process produces GPP and NPP regardless of the quality of the 8-day FPAR/LAI (MOD15A2) data, which may introduce considerable error in the 8-day MODIS GPP product and, therefore, annual GPP and NPP (Kang et al. 2005).
3. The C4 MOD17 BPLUT was primarily developed and tested before the MODIS launch using upstream inputs that differ from those used operationally (Running et al. 2000).
4. C4 MOD17 uses a fill value for all vegetated pixels rather than a calculated annual quality control (QC) assessment, because there were insufficient data at launch to establish meaningful annual QC values.

To solve the first problem, we have spatially interpolated coarse resolution GMAO data to the resolution of the 1-km MODIS pixel using a non-linear interpolation scheme. Our studies reveal that this spatial interpolation of GMAO can also improve the accuracy of daily meteorological inputs except remove the big GMAO foot print in GPP/NPP images (Zhao et al. 2005). To account for quality control issues in the MODIS FPAR/LAI product, we have temporally filled the missing and contaminated data in the 8-day FPAR/LAI profile for each MODIS pixel. As illustrated in Fig. 28.6, the 8-day MODIS FPAR/LAI data (Myneni et al. 2002) contain some cloud-contaminated or missing data. According to the MOD15A2 quality assessment scheme provided by Myneni et al. (2002), FPAR/LAI values retrieved by the main algorithm (i.e., a Radiation Transfer model, denoted as RT) are most reliable, and those retrieved by the back-up algorithm (i.e., the empirical relationship between FPAR/LAI and NDVI) are less reliable since the backup algorithm is employed mostly when cloud cover, strong atmospheric effects, or snow/ice are detected. The LAI retrievals from the backup algorithm are of lower quality and not suitable for validation and other studies (Yang et al. 2006). For the C4 products, LAI retrievals by the backup algorithm generally have higher values than those derived using the RT model (Yang et al. 2006). This explains why the filled LAI is well below the maxima in some periods, as shown in Fig. 28.6 for the Amazon. The temporal filling process entails two steps. If the first (or last) 8-day FPAR/LAI is unreliable or missing, it is replaced by the closest reliable 8-day (16-day) value during that calendar year. This step ensures that the second step is performed in which, the remaining unreliable FPAR/LAI data are replaced by linear interpolation of the nearest reliable values prior to and after the missing data point.

We have also retuned the BPLUT based on the MODIS GPP validation work on eddy flux towers (Turner et al. 2003b, 2005, 2006a, b; Heinsch et al. 2006), and the synthesized global NPP datasets for different biomes (Clark et al. 2001; Gower et al. 1997, 2001; Zheng et al. 2003) to address the third issue.

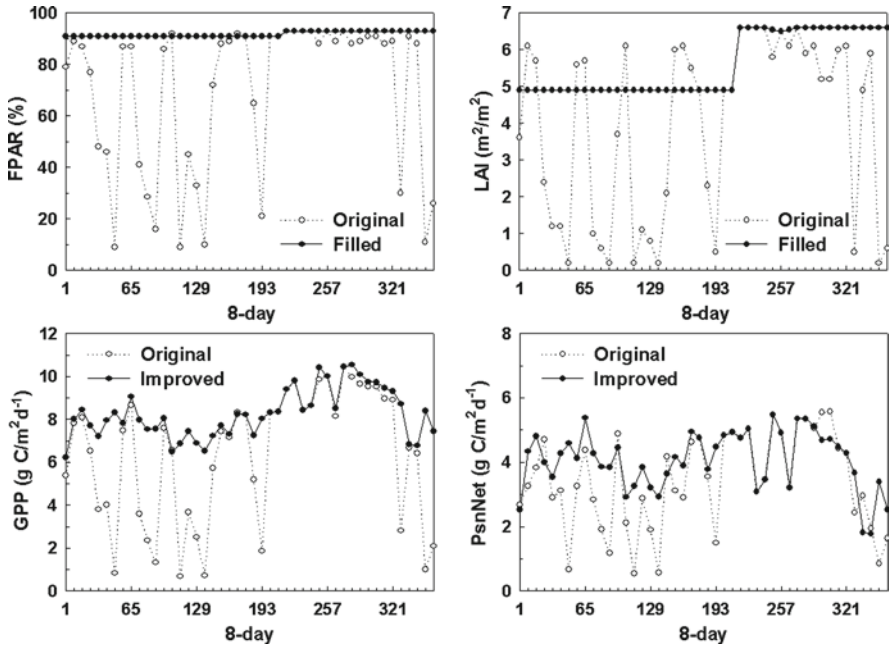


Fig. 28.6 An example depicting temporal filling unreliable 8-day Collection-4 FPAR/LAI, and therefore improved 8-day GPP and PsnNet for one MODIS 1-km pixel located in Amazon basin (lat = -5.0, lon = -65.0) (Zhao et al. 2005)

For the last issue regarding annual QC, we have created a meaningful annual GPP/NPP QC, expressed as:

$$QC = (NU_{g} / TOTAL_{g}) \times 100 \tag{28.8}$$

where NU_{g} is the number of days during the growing season with unreliable or missing MODIS LAI inputs, $TOTAL_{g}$ is total number of days in the growing season. The growing season is defined as all days for which T_{min} is greater than $-8^{\circ}C$, which is the minimum temperature control on photosynthesis for all biomes in the BPLUT. Although respiration can occur daily, T_{min} is below $-8^{\circ}C$, and both FPAR and LAI are perhaps greater than 0, the GPP magnitude is negligible during the non-growing season. Furthermore, since the annual QC definition is limited to data during the growing season, the number of unreliable LAI values caused by snow cover will contribute less to the QC than those caused by cloud cover. Therefore, the annual MOD17A3 QC reveals the number of growing days (%) when the FPAR/LAI were artificially filled because of cloud cover when calculating the 8-day GPP and annual GPP/NPP (Fig. 28.7). Details of the improvements are available in Zhao et al. (2005).

We have further improved the MOD17 algorithm for C5 based on new knowledge of the MODIS LAI, and plant maintenance respiration. The C4

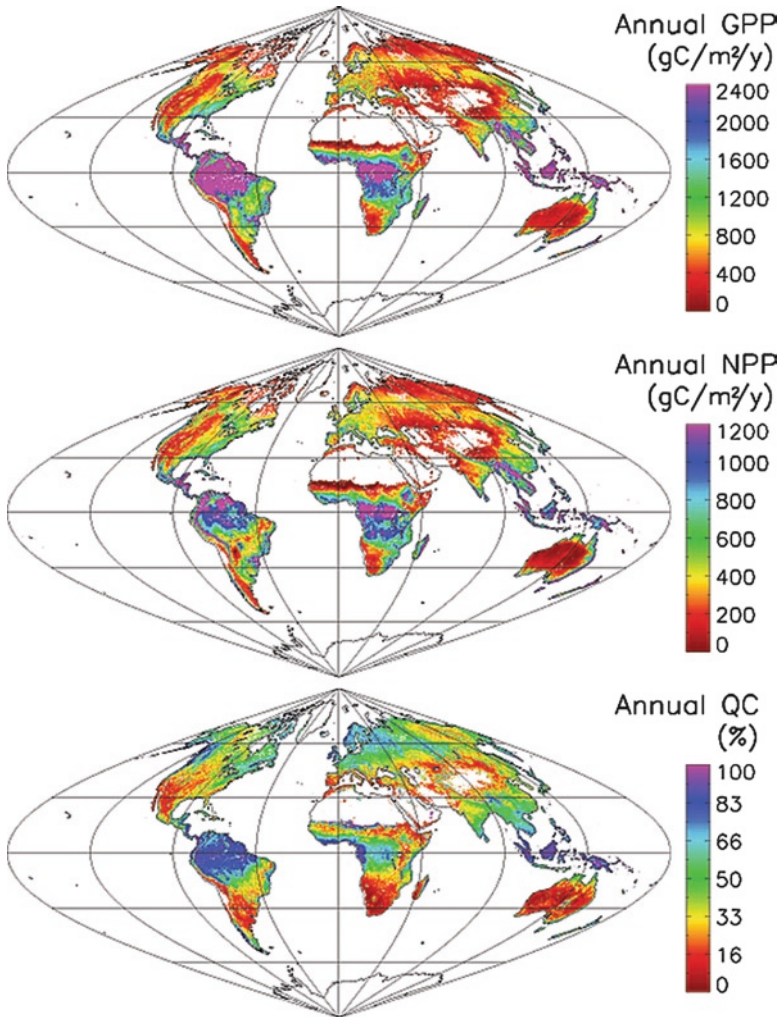


Fig. 28.7 Six-year (2000–2005) mean global 1-km C4.8 improved MODIS annual total GPP, NPP and annual QC images estimated with the C5 MOD17 system but with C4 MODIS FPAR/LAI input (annual QC denotes percent of 8-day with filled MOD15A2 FPAR/LAI as input to the improved MOD17 due to the cloud/aerosol contamination and missing periods. Also see the definition in (28.8) in the text). Land regions with *white color* are barren, sparsely vegetated and non-vegetated areas, including urban, snow and ice, and inland water body

MOD17 algorithm calculates growth respiration (R_g) using the annual maximum LAI (LAI_{max}), and thus, the accuracy of R_g is determined by the accuracy of LAI_{max} . However, when LAI is $>3.0 \text{ m}^2/\text{m}^2$, surface reflectances have lower sensitivity to LAI and the MODIS LAI is retrieved, in most cases, under reflectance saturation conditions (Myneni et al. 2002). Generally, annual MODIS LAI_{max} is calculated as $6.8 \text{ m}^2/\text{m}^2$ for pixels classified as forests. This logic can generate

R_g values that are greater than NPP. R_g is the energy cost for constructing organic compounds fixed by photosynthesis, and it is empirically parameterized as 25% of NPP (Ryan 1991; Cannell and Thornley 2000). To improve the algorithm, we replaced the LAI_{max} dependent R_g with $R_g = 0.25 \times NPP$, and annual MODIS NPP is computed as

$$NPP = GPP - R_m - R_g = GPP - R_m - 0.25 \times NPP \quad (28.9)$$

where R_m is plant maintenance respiration, and therefore,

$$\begin{aligned} NPP &= 0.8 \times (GPP - R_m) && \text{when } GPP - R_m \geq 0, \text{ and} \\ NPP &= 0 && \text{when } GPP - R_m < 0. \end{aligned} \quad (28.10)$$

Until recently, a constant value of 2.0 was widely used for Q_{10} in modelling R_m . Tjoelker et al. (2001) concluded that the Q_{10} for leaves declines linearly with increasing air temperatures in a consistent manner among a range of taxa and climatic conditions (see (28.7)). Wythers et al. (2005) found that the adoption of this temperature-variable Q_{10} may enhance the application of ecosystem models across broad spatial scales, or in climate change scenarios. We have adopted (28.6), replacing the constant Q_{10} for leaves in the algorithm to improve its performance.

28.6 Global Six-Year (2000–2005) Results

Using the improved algorithm and data processing, and the consistent GMAO data (version GEOS4), we reprocessed the global 1-km MOD17 for a six-year period (2000–2005). For this reprocessing, we have again retuned the BPLUT based on recent GPP validation efforts of the Bigfoot project and NTSG, as well as this consistent GMAO dataset. We have named the dataset Collection 4.8 (C4.8) MOD17, even though it was generated with our C5 system, because the input MODIS land cover is Collection-3 (C3) and the input MODIS FPAR/LAI is C4, which form the basis for our C4 processing. The following three sections present the results from the 6-year C4.8 GPP/NPP datasets.

28.6.1 Mean Annual GPP, NPP and QC

Figure 28.7 reveals the spatial pattern of the 6-year mean annual total GPP, NPP, and related QC. As expected, MODIS GPP and NPP have high values in areas covered by forests and woody savannas, especially in tropical regions. Low NPP occurs in areas dominated by adverse environments, such as high latitudes with

Table 28.1 Mean, standard deviation (in parentheses) of annual total GPP and NPP, and ratio of NPP to GPP for different biome types based on the 6-year (2000–2005) 1-km mean annual MODIS GPP and NPP, the corresponding areas for different biome types are derived from MODIS land cover

	Evergreen needle forests	Evergreen broadleaf forests	Deciduous needle forests	Deciduous broadleaf forests	Mixed forests	Closed shrublands
Area (M Km ²)	6.14	15.10	2.05	1.73	7.06	0.95
GPP (g C/m ² /yr)	834 (329)	2668 (342)	726 (140)	1276 (376)	1043 (380)	809 (359)
NPP (g C/m ² /yr)	464 (152)	1148 (301)	305 (64)	555 (229)	523 (187)	387 (190)
Ratio (NPP/GPP)	0.56	0.43	0.42	0.43	0.50	0.48
	Open shrublands	Woody Savannas	Savannas	Grasslands	Croplands	
Area (M Km ²)	27.49	9.28	9.74	10.70	19.53	
GPP (g C/m ² /yr)	309 (209)	1368 (533)	1208 (417)	392 (262)	765 (310)	
NPP (g C/m ² /yr)	145 (108)	670 (276)	596 (257)	201 (122)	419 (150)	
Ratio (NPP/GPP)	0.47	0.49	0.49	0.51	0.55	

Note: Barren or sparsely vegetated land areas are excluded

short growing seasons constrained by low temperatures, and dry areas with limited water availability. At the global scale, from 2000 to 2005, MODIS estimated a total terrestrial annual GPP of 109.07 Pg C (± 1.66 S.D.), and an annual NPP of 52.03 Pg C (± 1.17 S.D.), ignoring barren land cover as defined by the MODIS land cover product. For vegetated areas, the mean annual GPP and NPP are 996.03 (± 823.67 S.D.) and 475.19 (± 375.44 S.D.) g C/m²/yr, respectively. Table 28.1 lists the mean and standard deviation of annual total GPP, NPP and the ratio between the two for different biome types and their corresponding areas. Evergreen broadleaf forests have the highest GPP and NPP, while open shrublands have the lowest. Generally, NPP is approximately half of GPP, agreeing with the results from field observations (Waring et al. 1998; Gifford 2003). The QC image reflects the percent of filled FPAR/LAI during the growing season as discussed above, and as expected, high values occur in areas of frequent cloud cover (i.e., higher precipitation).

28.6.2 Seasonality

The 8-day composite MOD17 GPP also demonstrates the seasonality of terrestrial ecosystem uptake of carbon from the atmosphere by photosynthesis at the 1-km scale. Figure 28.8 illustrates the seasonality of GPP both spatially and temporally. We have aggregated 8-day values to 3 months (Fig. 28.8a). The spatial seasonal variations clearly demonstrate the expected peak GPP in summer and the low values in winter over the mid- and high-latitudes of the Northern Hemisphere (NH). For Africa, the temporal development of MODIS GPP corresponds spatially to the movements of the Intertropical Convergence Zone (ITCZ). The dry season (approximately July) has lower GPP than the wet periods for the African rain forests south

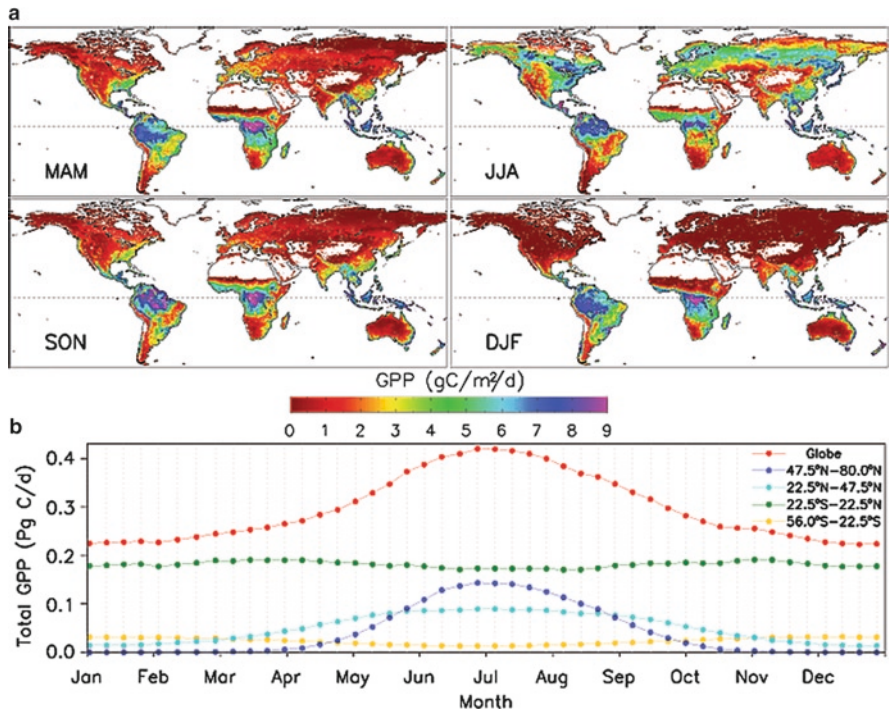


Fig. 28.8 Spatial pattern of (a) the seasonality of MODIS GPP and (b) temporal annual cycle of GPP at 8-day interval for four latitude bands and the globe. Land regions with white color are barren, sparsely vegetated and non-vegetated areas, including urban, snow and ice, and inland water bodies

of equator, because, compared with rainforests on other continents, the African tropical rainforest is relatively dry and receives $1,600\text{--}2,000\text{ mm/year}^{-1}$ of rainfall, while areas receiving more than 3,000 mm of rainfall in a given year are largely confined to the coastal areas of Upper and Lower Guinea. Virtually nowhere in the African tropical rainforest is the mean monthly rainfall higher than 100 mm for any month during the year (Tucker et al.). Rainforests of the Amazon basin have higher GPP during the dry season from July to November than during the wet season, which agree with Huete et al. (2006). During the dry season, monthly precipitation in the Amazon basin is approximately 100 mm, making solar radiation, not water, the leading limiting factor in this region. Figure 28.8b shows the annual cycle of total GPP for four latitudinal bands and for the entire globe. Relatively strong seasonal signals occur for the mid- and high-latitudes of the NH (i.e., north of 22.5°N). The areas south of 22.5°S have opposite seasonal profiles relative to the mid- and high-latitudes of NH, and the seasonality for the southern hemisphere is much weaker. For the entire tropical region ($22.5^\circ\text{S}\text{--}22.5^\circ\text{N}$), there is little to no seasonality, while total GPP is always the highest among the four latitude bands. Therefore, at the global scale, magnitudes of the annual GPP cycle are mostly attributed to the tropical region, while the seasonality is largely determined by areas north of 22.5°N .

With global warming, the growing season in high latitudes has lengthened (Myneni et al. 1997; Zhou et al. 2001), and the 8-day MOD17 is a valuable dataset to detect the resulting change in the amount of carbon uptake.

28.6.3 Interannual Variability

The improved C4.8 MOD17 also has the ability to capture the response of terrestrial ecosystems to extreme climatic variability at the regional scale, especially widespread drought. During the growing season, water stress is generally the leading control factor on GPP and NPP. Figure 28.9 shows NPP anomalies from 2000 to 2005 as estimated from the 1-km C4.8 improved MODIS NPP, which demonstrates the sensitive responses of terrestrial ecosystem to drought in both China and the southwestern United States during 2000, Europe in 2003, and Australia and the Amazon in 2005. In 2000, the drought occurring in both China and the southwestern USA had negative impacts on NPP. The severe drought in Australia and a large part of the USA in 2002 led to reduced NPP. During 2003 the heat wave in Europe led to drought, and lowered NPP in the region. In 2005, the Amazon experienced the worst drought in 100 years, making water availability the leading limiting factor instead of solar radiation as

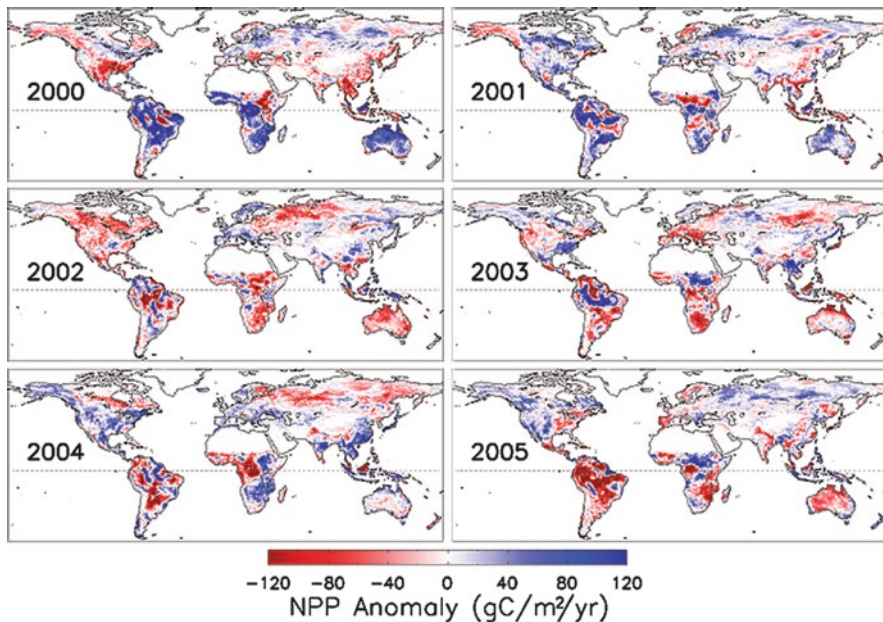


Fig. 28.9 Spatial pattern of C4.8 improved 1-km MODIS NPP anomalies from 2000 to 2005 with same period as the baseline for average. Land regions with *white color* are barren, sparsely vegetated and non-vegetated areas, including urban, snow and ice, and inland water bodies

found by Nemani et al. (2003) and Huete et al. (2006) under normal conditions. Australia also experienced drought in 2005, which is captured by MODIS NPP anomalies. The above-mentioned droughts are reported by different news media and scientific journals. While unable to monitor the impacts of climatic anomaly on ecosystems at the stand or local level, the 1-km resolution MOD17 can measure and track the changes in environment, such as desertification, deforestation, disturbance (e.g., fire and insect outbreak), and the impacts of pollution on a larger scale.

Using AVHRR to calculate NPP, Nemani et al. (2003) found that during the period between 1982 and 1999, the correlation between NPP and inverted anomaly of CO_2 interannual growth rate was 0.70 ($P < 0.001$). For this improved 1-km MOD17, the correlation between MODIS NPP and inverted anomaly of CO_2 interannual growth rate is 0.85 ($P < 0.016$), and 0.91 for the NCEP-driven MODIS NPP with CO_2 growth rate (Fig. 28.10). The high correlation between NPP and CO_2 growth rates may imply terrestrial NPP, rather than heterotrophic respiration or wildfires, is the primary driver of atmospheric CO_2 growth rates. Several potential reasons account for this. First, the similar variations of global rates of changes in $^{13}\text{C}/^{12}\text{C}$ isotopic ratio of CO_2 and CO_2 suggest that exchange of atmospheric CO_2 with terrestrial plants and soil is the dominant cause for both signals (Keeling et al. 2001). Second, tropical NPP values are more highly correlated with CO_2 growth rates than at other latitudes, and NPP and soil respiration are more tightly coupled in tropical areas (Nemani et al. 2003). Third, soil carbon residence times range from less than 4 years in hot, wet tropical areas to greater than 1,000 years in cold boreal or dry desert conditions (Barrett 2002; Mayorga et al. 2005), and furthermore, NPP is the source of soil respiration, and thus, to some extent, NPP exerts control over heterotrophic respiration. More studies are needed to quantify the

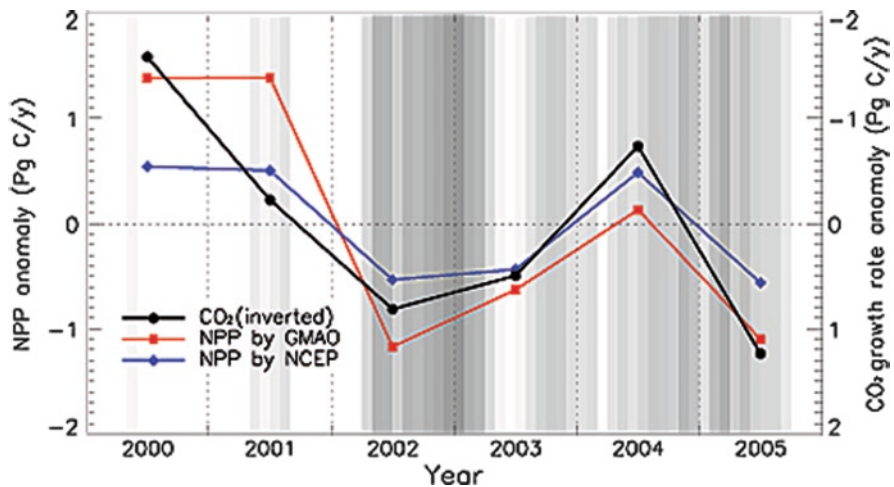


Fig. 28.10 Interannual variations in global total C4.8 MOD17 NPP driven by NCEP and GMAO, respectively, in relation to inverted atmospheric CO_2 interannual growth rate. A Multivariate ENSO Index (MEI) is shown in gray scale, where darker shades represent higher MEI values

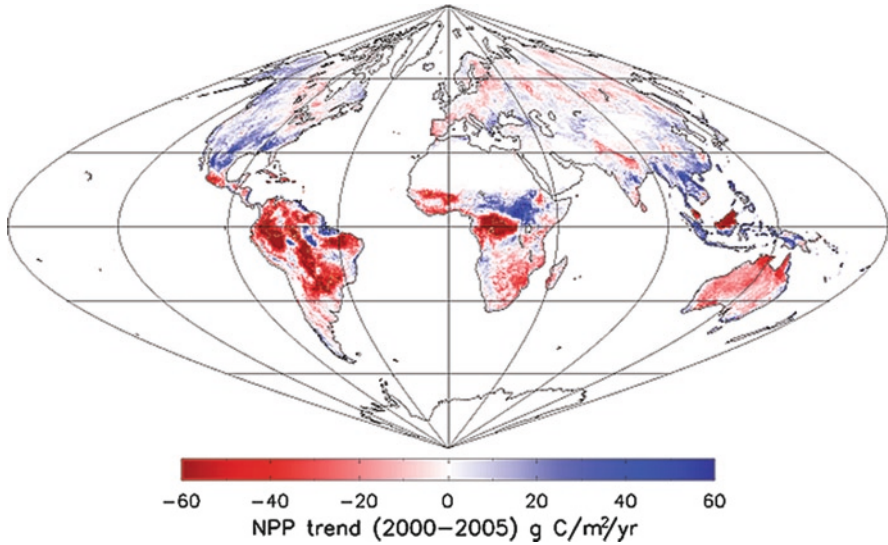


Fig. 28.11 Spatial pattern of 1-km NPP trend from 2000 to 2005 estimated by C4.8 MOD17. Land regions with *white color* are barren, sparsely vegetated and non-vegetated areas, including urban, snow and ice, and in-land water bodies. Some *white color* includes areas with NPP trend close to 0

contribution of terrestrial NPP to the variation in atmospheric CO_2 in the context of the global carbon cycle.

The 6 years of MODIS data, on the other hand, show that global total NPP decreased during 2000–2005 (Fig. 28.10). Spatially, the largest decreasing trends occurred in areas of the tropics and most of Southern Hemisphere, while increasing trends in most of mid-latitudes over the Northern Hemisphere (Fig. 28.11).

28.7 Land Management and Biospheric Monitoring Applications

MODIS NPP is potentially very useful for land management and renewable natural resource estimations. MODIS weekly GPP agreed well with field-observed herbaceous biomass for a grassland in North Dakota (Reeves et al. 2006), and was strongly related to wheat yield for cropland in Montana (Reeves et al. 2005). For forests in the Mid-Atlantic region of the U.S., the regional mean of MODIS NPP was very close to the mean stem and root increment estimated from the US Forest Service Forest Inventory and Analysis (FIA) data (Pan et al. 2006).

MODIS NPP products are also invaluable to measure both changes in the environment, such as desertification, deforestation, disturbances (e.g., fire and insect outbreak), as well as the impacts of pollution and climate change, and to evaluate ecosystem status and service (e.g., ecosystem health, habitat and wildlife, ecological

footprint) (Running et al. 2004). Loehman (2006) used MODIS GPP to study the impacts of resources on rodent populations, especially deer mice, the main reservoir host for the Sin Nombre virus (SNV), a primary disease agent of Hantavirus pulmonary syndrome. Milesi et al. (2003a, b, 2005) have used the global remotely-sensed NPP to analyze the policy relevance of NPP, such as the effects of urbanization on NPP, and identification of human populations that are vulnerable to changes in NPP resulting from interannual climate variability. In addition, MODIS NPP data can provide information to policy makers and stakeholders in evaluating greenhouse gas mitigation (Baisden 2006). Finally, the Heinz Center is considering MODIS annual NPP as a measure of national ecosystem services (Meyerson et al. 2005).

We now use the MODIS GPP and NPP algorithm and data to develop a real-time biospheric monitoring system. The final goal of MOD17 is to generate a regular, real-time monitor of the terrestrial biosphere that provides a meaningful quantification of ecosystem biogeochemistry, of which GPP and NPP are the best current candidates. However, few scientists, and even fewer policy makers can relate intuitively to weekly maps with units of “gC/m²/d”. Departures from a long-term mean condition (similar to weather data) is the most easily understood and interpreted presentation of MODIS GPP and NPP data for policy purposes. With a defined high-quality historical average GPP for each 1-km pixel now complete for 2000–2005, we can compare the most recent 32-day MOD17 GPP against the average GPP for the same period from 2000 to 2005 as an anomaly map. At the global scale (Fig. 28.12), we will use the coarse resolution NCEP/NCAR re-analyses data to generate near real-time GPP. For North America, relatively high resolution, i.e., 32-km, near real-time weather data are available from the regional data assimilation

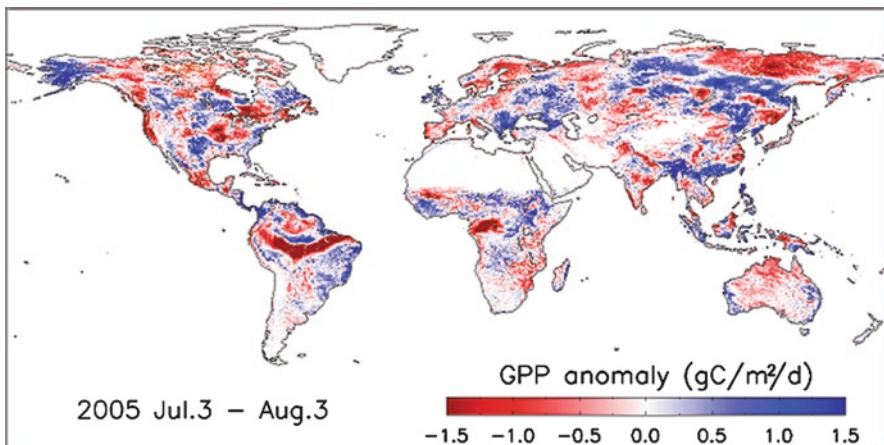


Fig. 28.12 A prototype observed departure from normal for 32-day GPP. When operational, this map updates every 32 days (less than 8 days behind the acquisition date). Land regions with *white color* are barren, sparsely vegetated and non-vegetated areas, including urban, snow and ice, and inland water bodies. Some *white color* includes areas with GPP anomaly close to 0

system for the North American Regional Reanalysis (NARR) (Mesinger et al. 2006), or our own surface observation gridding system (SOGS) (Jolly et al. 2005b) using real-time observations from National Climatic Data Center (NCDC) to produce relatively high resolution real-time MODIS GPP and NPP. Nemani's Ecocasting System (<http://ecocast.arc.nasa.gov/>) will use this real-time GPP for future forecasting.

Anomalies in terrestrial GPP and NPP demonstrate the effects of environmental drivers such as ENSO events, climate change, pollution episodes, land degradation, and agricultural expansion. A regular dataset for global GPP, NPP and their anomalies and trends are useful in biodiversity analysis (Sala et al. 2000; Waring et al. 2006) and as an environmental monitor for policy formulation (Niemeijer 2002). These anomalies delivered in near real-time will provide important information on global agricultural commodity trends. This includes similar yet improved information over what currently are evaluated with AVHRR NDVI by the Foreign Agricultural Service of the U.S. Dept of Agriculture, the FAO, and other agencies. The United Nations FAO is currently considering MODIS GPP anomaly dataset for a new global Drought and Famine warning system. The GEOSS (Global Earth Observation System of Systems) requires quantitative monitoring of the global biosphere with sufficient temporal continuity for change detection, similar to what is offered here with the MODIS NPP and evapotranspiration multi-year datasets. More discussion of MOD17 applications are found in Running et al. (2004).

28.8 Future Directions

Water stress is one of the most important limiting factors controlling terrestrial primary production, and the performance of a primary production model is largely determined by its capacity to capture environmental water stress. The MOD17 GPP and NPP algorithm uses only VPD to express total environmental water stress. In some dry regions where soil water is severely limiting, MOD17 underestimates water stress, thus overestimating GPP, and fails to capture the intra-annual variability of water stress for areas with strong summer monsoons (Mu et al. 2006a; Turner et al. 2005; Leuning et al. 2005; Pan et al. 2006). We have developed a MODIS ET algorithm, validated at 22 AmeriFlux towers, and generated a global MODIS evapotranspiration product (Mu et al. 2006b). Once the MODIS ET has reached Stage-2 validation, we will add ET as an additional modifier to the ϵ calculation at each 8-day time step. Since this index represents a non-linear relationship between soil moisture and leaf water potential, we expect the final relationship will manifest non-linear as well.

With the Terra and Aqua satellites nearing the end of their missions, spectral data from the next-generation radiometer, the Visible-Infrared Imager-Radiometer Suite (VIIRS) flying on the National Polar-orbiting Operational Environmental Satellite System (NPOESS) (Miller et al. 2006), is expected to generate MOD17-like products. The MOD17 algorithm can also use data from other environmental satellites launched by different countries to produce regional or global GPP and NPP. At that point, we

expect these weekly GPP and annual NPP data to routinely become part of land management, environmental policy analysis, agricultural economics, and monitoring of biospheric change. These data products do not meet all the needs and expectations of scientists, managers, policymakers, and the public. However, they are unique tools, which provide global coverage and weekly continuity of key measures of the impacts of environmental changes on terrestrial activity, and ultimately, on humankind.

Acknowledgments This research was funded by the NASA/EOS MODIS Project (NNG04HZ19C) and Natural Resource/Education Training Center (grant NAG5-12540). The improved 1-km MODIS terrestrial GPP and NPP data are available at <http://www.nts.gov.umt.edu/>. We thank Dr. Niall Hanan for his thoughtful and insightful comments on an earlier draft of this paper.

References

- Abuelgasim AA, Fernandes RA, Leblanc SG (2006) Evaluation of national and global LAI products derived from optical remote sensing instruments over Canada. *IEEE Trans Geosci Remote Sens* 44(4):1872–1884
- Amthor JS (2000) The Mccree–de Wit–Penning de Vries–Thornley respiration paradigms: 30 years later. *Ann Bot (Lond)* 86:1–20
- Baisden WT (2006) Agriculture and forest productivity for modelling policy scenarios: evaluating approaches for New Zealand greenhouse gas mitigation. *J R Soc N Z* 36:1–15
- Baldocchi D, 26 co-authors (2001) FLUXNET: A new tool to study the temporal and spatial variability of ecosystem-scale carbon dioxide, water vapor and energy flux densities. *Bull Amer Meteorol Soc* 82:2415–2434
- Barrett DJ (2002) Steady state turnover time of carbon in the Australian terrestrial biosphere. *Global Biogeochem Cycles* 16. doi:10.1029/2002GB001860
- Cannell MGR, Thornley JHM (2000) Modelling the components of plant respiration: some guiding principles. *Ann Bot (Lond)* 85:45–54
- Churkina G, Running SW (1998) Contrasting climatic controls on the estimated productivity of different biomes. *Ecosystems* 1:206–215
- Clark DA, Brown S, Kicklighter D, Chambers J, Thomlinson JR, Ni J, Holland EA (2001) Net Primary Production in tropical forests: an evaluation and synthesis of existing field data. *Ecol Appl* 11:371–384
- Cohen WB, Maersperger TK, Turner DP, Ritts WD, Pflugmacher D, Kennedy RE, Kirschbaum A, Running SW, Costa M, Gower ST (2006) MODIS land cover and LAI Collection 4 product quality across nine sites in the Western Hemisphere. *IEEE Trans Geosci Remote Sens* 44(7):1843–1857
- Cohen WB, Maersperger TK, Yang Z, Gower ST, Turner DP, Ritts WD, Berterretche M, Running SW (2003) Comparisons of land cover and LAI estimates derived from ETM+ and MODIS for four sites in North America: a quality assessment of 2000/2001 provisional MODIS products. *Remote Sens Environ* 88:221–362
- Falge E, 31 co-authors (2002) Seasonality of ecosystem respiration and gross primary production as derived from FLUXNET measurements. *Agric For Meteorol* 113:75–95
- Gower ST, Krankina O, Olson RJ, Apps MJ, Linder S, Wang C (2001) Net primary production and carbon allocation patterns of boreal forest ecosystems. *Ecol Appl* 11:1395–1411
- Gower ST, Vogel JG, Norman JM, Kucharik CJ, Steele SJ, Stow TK (1997) Carbon distribution and aboveground net primary production in aspen, jack pine, and black spruce stands in Saskatchewan and Manitoba, Canada. *J Geophys Res* 104(D22):29029–29041
- Gifford RM (2003) Plant respiration in productivity models: Conceptualisation, representation and issues for global terrestrial carbon-cycle research. *Funct Plant Biol* 30:171–186

- Heinsch FA, 12 co-authors (2003) User's Guide: GPP and NPP (MOD17A2/A3) Products, NASA MODIS Land Algorithm. University of Montana, NTSG, 57
- Heinsch FA, 25 co-authors (2006) Evaluation of remote sensing based terrestrial productivity from MODIS using ameriflux tower eddy flux network observations. *IEEE Trans Geosci Remote Sens* 44:1908–1925
- Huete AR, Didan K, Shimabukuro YE, Ratana P, Saleska SR, Hutrya LR, Yang W, Nemani RR, Myneni R (2006) Amazon rainforests green-up with sunlight in dry season. *Geophys Res Lett* 33:L06405, doi:10.1029/2005GL025583
- Imhoff ML, Bounoua L, Richetts T, Loucks C, Harriss R, Lawrence WT (2004) Global pattern in human consumption of net primary production. *Nature* 429:870–873
- Jolly WM, Nemani R, Running SW (2005a) A generalized, bioclimatic index to predict foliar phenology in response to climate. *Glob Change Biol* 11:619–632
- Jolly WM, Graham JM, Nemani RR, Running SW (2005b) A flexible, integrated system for generating meteorological surfaces derived from point sources across multiple geographic scales. *Environ Model Software* 20:873–882
- Justice CO, Townshend JRG, Vermote EF, Masuoka E, Wolfe RE, Saleous N, Roy DP, Morisette JT (2002) An overview of MODIS Land data processing and product status. *Remote Sens Environ* 83:3–15
- Kang S, Running SW, Zhao M, Kimball JS, Glassy J (2005) Improving continuity of MODIS terrestrial photosynthesis products using an interpolation scheme for cloudy pixels. *Int J Remote Sens* 28:1659–1676
- Keeling CD, Piper SC, Bacastow RB, Wahlen M, Whorf TP, Heimann M, Meijer HA (2001) Exchanges of atmospheric CO₂ and ¹³CO₂ with the terrestrial biosphere and oceans from 1978 to 2000: 1. Global aspects, SIO Reference Series, 01–06 Scripps Institution of Oceanography, San Diego
- Leuning R, Cleugh HA, Zegelin SJ, Hughes DE (2005) Carbon and water fluxes over a temperate Eucalyptus forest and a tropical wet/day savanna in Australia: measurements and comparison with MODIS remote sensing estimates. *Agric For Meteorol* 129:151–173
- Loehman R (2006) Modeling interactions among climate, landscape, and emerging diseases: a hantavirus case study. Ph.D. dissertation, University of Montana
- Mayorga E, Aufdenkampe AK, Masiello CA, Krusche AV, Hedges JI, Quay PD, Richey JE, Brown TA (2005) Young organic matter as a source of carbon dioxide outgassing from Amazonian rivers. *Nature* 436:538–541
- Melillo JM, McGuire AD, Kicklighter DW, Moore B III, Vorosmarty CJ, Schloss AL (1993) Global climate change and terrestrial net primary production. *Nature* 63:234–240
- Mesinger F, 18 co-authors (2006) North American regional reanalysis. *Bull Amer Meteorol Soc* 87:343–360
- Meyerson L, Baron J, Melillo J, Naiman R, O'Malley R, Orians G, Palmer M, Pfaff A, Running S, Sala O (2005) Aggregate measures of ecosystem services: Can we take the pulse of nature? *Front Ecol Environ* 3:56–59
- Milesi C, Elvidge CD, Nemani RR, Running SW (2003a) Assessing the impact of urban land development on net primary productivity in the southeastern United States. *Remote Sens Environ* 86:273–432
- Milesi C, Elvidge CD, Nemani RR, Running SW (2003b) Assessing the environmental impacts of human settlements using satellite data. *Manage Environ Qual* 14:99–107
- Milesi C, Hashimoto H, Running SW, Nemani RR (2005) Climate variability, vegetation productivity and people at risk. *Global Planet Change* 47:221–231
- Miller SD, Hawkins JD, Kent J, Turk FJ, Lee TF, Kuciauskas AP, Richardson K, Wade R, Hoffman C (2006) Nexsat: Previewing NPOESS/VIIRS Imagery Capabilities. *Bull Amer Meteorol Soc* 87:433–446
- Monteith JL (1972) Solar radiation and productivity in tropical ecosystems. *J Appl Ecol* 9: 747–766
- Monteith JL (1977) Climate and efficiency of crop production in Britain. *Philos Trans R Soc Lond B* 281:277–294

- Mu Q, Zhao M, Heinsch FA, Liu M, Tian H, Running SW (2006a) Evaluating water stress controls on primary production in biogeochemical and remote sensing-based models. *J Geophys Res* 112:G01012, doi:10.1029/2006JG000179
- Mu Q, Heinsch FA, Zhao M, Running SW, Cleugh HA, Leuning R (2006b) Development of a global evapotranspiration algorithm based on MODIS and global meteorology data. *Remote Sens Environ* 111(4):519–536
- Myneni RB, Keeling CD, Tucker CJ, Asrar G, Nemani RR (1997) Increased plant growth in the northern high latitudes from 1981–1991. *Nature* 386:698–702
- Myneni RB, 15 co-authors (2002) Global products of vegetation leaf area and fraction absorbed PAR from year one of MODIS data. *Remote Sens Environ* 83:214–231
- Wythers KR, Reich P, Tjoelker MG, Bolstad PB (2005) Foliar respiration acclimation to temperature and temperature variable Q_{10} alter ecosystem carbon balance. *Glob Change Biol* 11:435–449
- Nemani RR, Keeling CD, Hashimoto H, Jolly WM, Piper SC, Tucker CJ, Myneni RB, Running SW (2003) Climate-driven increases in global terrestrial net primary production from 1982 to 1999. *Science* 300:1560–1563
- Niemeijer D (2002) Developing indicators for environmental policy: data-driven and theory-driven approaches examined by example. *Environ Sci Policy* 5:91–103
- Pan Y, Birdsey R, Hom J, McCullough K, Clark K (2006) Improved estimates of net primary productivity from MODIS satellite data at regional and local scales. *Ecol Appl* 16:125–132
- Pandya MR, Singh RP, Chaudhari KN, Bairagi GD, Sharma BR, Dadhwal VK, Parihar JS (2006) Leaf area index retrieval using IRS LISS-III sensor data and validation of the MODIS LAI product over central India. *IEEE Trans Geosci Remote Sens* 44:1858–1865
- Prentice IC, Farquhar GD, Fasham MJR, Goulden ML, Heimann M, Jaramillo VJ, Khashgi HS, Le Quéré C, Scholes RJ, Wallace DWR (2001) The carbon cycle and atmospheric carbon dioxide. In: Ding JY, Griggs DJ, Noguer M, van der Linden PJ, Dai X, Maskell K, Johnson CA (eds) *Climate change 2001: the scientific basis. Contribution of working group I to the third assessment report of the intergovernmental panel on climate change*. Cambridge University Press, Cambridge, United Kingdom and New York, USA, T. Houghton, 182–237
- Reeves MC, Zhao M, Running SW (2005) Usefulness and limits of MODIS GPP for estimating wheat yield. *Int J Remote Sens* 27:1403–1421
- Reeves MC, Zhao M, Running SW (2006) Applying improved estimates of MODIS productivity to characterize grassland vegetation dynamics. *Rangeland Ecol Manage* 59:1–10
- Reichstein M, Valentini R, Running SW, Tenhunen J (2004) Improving remote sensing-based GPP estimates (MODIS-MOD17) through inverse parameter estimation with CARBOEUROPE eddy covariance flux data. *EGU meeting Nice 2004. Geophys Res Abstr* 6:01388
- Running SW, Hunt ER (1993) Generalization of a forest ecosystem process model for other biomes, BIOMEBGC, and an application for global-scale models. In: Ehleringer JR, Field CB (eds) *Scaling physiological processes: leaf to globe*. Academic Press, San Diego, pp 141–158
- Running SW, Nemani RR, Heinsch FA, Zhao M, Reeves M, Hashimoto H (2004) A continuous satellite-derived measure of global terrestrial primary productivity: Future science and applications. *Bioscience* 56:547–560
- Running SW, Baldocchi DD, Turner DP, Gower ST, Bakwin PS, Hibbard KA (1999) A global terrestrial monitoring network integrating tower fluxes, flask sampling, ecosystem modeling and EOS satellite data. *Remote Sens Environ* 70:108–128
- Running SW, Thornton PE, Nemani RR, Glassy JM (2000) Global terrestrial gross and net primary productivity from the earth observing system. In: Sala O, Jackson R, Mooney H (eds) *Methods in Ecosystem Science*. Springer-Verlag, New York, pp 44–57
- Ryan MG (1991) The effects of climate change on plant respiration. *Ecol Appl* 1:157–167
- Sala OE, 18 co-authors (2000) Global biodiversity scenarios for the year 2100. *Science* 287:1770–1774
- Schimel DS, 29 co-authors (2001) Recent patterns and mechanisms of carbon exchange by terrestrial ecosystems. *Nature* 414:169–172

- Strahler AH, Friedl M, Zhang X, Hodges J, Cooper CSA, Baccini A (2002) The MODIS land cover and land cover dynamics products Presentation at Remote Sensing of the Earth's Environment from Terra in L'Aquila, Italy
- Tjoelker MG, Oleksyn J, Reich P (2001) Modelling respiration of vegetation: evidence for a general temperature-dependent Q_{10} . *Glob Change Biol* 7:223–230
- Tucker CJ, Townshend JRG, Goff TE (1985) African land-cover classification using satellite data. *Science* 227:369–375
- Turner DP, Ritts WD, Zhao M, Kurc SA, Dunn AL, Wofsy SC, Small EE, Running SW (2006a) Assessing interannual variation in MODIS-based estimates of gross primary production. *IEEE Trans Geosci Remote Sens* 44:1899–1907
- Turner DP, Ritts WD, Cohen WB, Gower ST, Running SW, Zhao M, Costae MH, Kirschbaum AA, Ham JM, Saleska SS, Ahl DE (2006b) Evaluation of MODIS NPP and GPP products across multiple biomes. *Remote Sens Environ* 102:282–292
- Turner DP, Urbanski S, Bremer D, Wofsy SC, Meyers T, Gower ST, Gregory M (2003a) A cross-biome comparison of daily light use efficiency for gross primary production. *Glob Change Biol* 9:383–395
- Turner DP, Ritts WD, Cohen WB, Gower ST, Zhao M, Running SW, Wofsy SC, Urbanski S, Dunn SA, Munger JW (2003b) Scaling Gross Primary Production (GPP) over boreal and deciduous forest landscapes in support of MODIS GPP product validation. *Remote Sens Environ* 88:256–270
- Turner DP, 17 co-authors (2005) Site-level evaluation of satellite-based global terrestrial gross primary production and net primary production monitoring. *Glob Change Biol* 11:666–684
- Wang Y, Woodcock CE, Buermann W, Stenberg P, Voipio P, Smolander H, Häme T, Tian Y, Hu J, Knyazikhin Y, Myneni RB (2004) Evaluation of the MODIS LAI algorithm at a coniferous forest site in Finland. *Remote Sens Environ* 91:114–127
- Waring RH, Landsberg JJ, Williams M (1998) Net primary production of forests: a constant fraction of gross primary production? *Tree Physiol* 18:129–134
- Waring RH, Coops NC, Fan W, Nightingale JM (2006) MODIS enhanced vegetation index predicts tree species richness across forested ecoregions in the contiguous U.S.A. *Remote Sens Environ* 103:218–226
- Yang W, Huang D, Tan B, Stroeve JC, Shabanov NV, Knyazikhin Y, Nemani RR, Myneni RB (2006) Analysis of leaf area index and fraction of PAR absorbed by vegetation products from the terra MODIS sensor: 2000–2005. *IEEE Trans Geosci Remote Sen* 44:1829–1842
- Zhao M, Heinsch FA, Nemani RR, Running SW (2005) Improvements of the MODIS terrestrial gross and net primary production global dataset. *Remote Sens Environ* 95:164–176
- Zhao M, Running SW, Nemani RR (2006) Sensitivity of Moderate Resolution Imaging Spectroradiometer (MODIS) terrestrial primary production to the accuracy of meteorological reanalyses. *J Geophys Res* 111:G01002. doi:10.1029/2004JG000004
- Zheng D, Prince S, Wright R (2003) Terrestrial net primary production estimates for 0.5° grid cells from field observations – a contribution to global biogeochemical modeling. *Glob Change Biol* 9:46–64
- Zhou L, Tucker CJ, Kaufmann RK, Slayback D, Shabanov NV, Myneni RB (2001) Variations in northern vegetation activity inferred from satellite data of vegetation index during 1981 to 1999. *J Geophys Res* 106:20069–20083